Erosion-induced carbon redistribution, burial and mineralisation — is the episodic nature of erosion processes important?

Peter Fiener, V. Dlugoß, K. Van Oost

Angaben zur Veröffentlichung / Publication details:

Fiener, Peter, V. Dlugoß, and K. Van Oost. 2015. "Erosion-induced carbon redistribution, burial and mineralisation — is the episodic nature of erosion processes important?" CATENA 133: 282–92. https://doi.org/10.1016/j.catena.2015.05.027.

Erosion-induced carbon redistribution, burial and mineralisation — Is the episodic nature of erosion processes important?

Fiener P. [a,*,1], Dlugoß V. [b,1], Van Oost K. [c]

[a] Institut für Geographie der Universität Augsburg, Germany
[b] Geographisches Institut der Universität zu Köln, Germany
[c] Earth & Life Institute, TECLIM, Université catholique de Louvain, Louvain-la-Neuve, Belgium

Keywords:
Soil organic carbon
Soil erosion
Erosion modelling
Carbon fluxes
CO_2

A B S T R A C T

There is still an ongoing scientific discussion regarding the importance of erosion-induced lateral soil organic carbon (SOC) redistribution for the burial and/or mineralisation of carbon and the resulting long-term C balance at the catchment scale. Especially the effects of the event driven nature of water erosion and the potentially associated enrichment of SOC in sediment delivery are still unclear. In general, two processes lead to enrichment of SOC: (i) enrichment due to selective interrill erosion at erosion sites, and (ii) enrichment due to selective depletion at deposition sites. In this study, the conceptual soil erosion and SOC turnover model SPEROS-C was adapted to integrate these processes and applied in a small arable catchment (4.2 ha) in Germany for a 57-year period. A total number of 901 model runs were performed with different realisations of frequency and magnitude of water erosion as well as realisations of enrichment and depletion ratios taken from literature and compared to a reference model run representing mean annual erosion without enrichment processes. In general, our modelling study indicates that ignoring temporal variability and enrichment processes may lead to a substantial misinterpretation of erosion-induced C fluxes. Especially the vertical C flux (difference between C inputs from plant assimilates and organic fertilizer and SOC mineralisation) at deposition sites strongly depends on the model parameterisation ranging from a maximum C source of −336 g C m^{-2} to a maximum C sink of 44 g C m^{-2}. In combination with a substantially higher C export due to enrichment processes, the overall C balance of the catchment potentially turns into a maximum C source of −44 g C m^{-2} at the end of the simulation period compared to a C source of −1 g C m^{-2} for the reference run.

1. Introduction

There is a growing interest in the lateral redistribution of soil organic carbon (SOC) due to erosion processes and their effects on landscape scale carbon burial or mineralisation (Berhe et al., 2008; Doetterl et al., 2013; Dymond, 2010; Fiener et al., 2012; Quinton et al., 2010; Van Oost et al., 2007). A general challenge in this research field is the event-driven nature of water erosion processes (Fiener and Auerswald, 2007; Nearing et al., 1999) governing short-term effects of erosion, transport, and deposition of SOC on vertical C (carbon) fluxes (difference between C inputs from plant assimilates and organic fertilizer and SOC mineralisation) (scale: minutes to days), and long-term effects by building up three-dimensional patterns of total SOC and also specific SOC pools within our landscapes (scale: decades to centuries). Some research focuses on the event-based lateral fluxes of soil and SOC and more rarely its associated short-term C effluxes to the atmosphere (Bremenfeld et al., 2013; Van Hemelryck et al., 2010a, 2010b; Wang et al., 2014), while other studies use long-term patterns in SOC in conjunction with long-term erosion studies, mostly based on erosion tracers (e.g. ^{137}Cs) or soil truncation, to evaluate the long-term effect of erosion on the C balance (Afshar et al., 2010; Doetterl et al., 2013; Martinez et al., 2010; Quine and Van Oost, 2007). Catchment scale patterns in SOC distributions are also the basis for developing and testing coupled soil erosion and C turnover models (Dlugoß et al., 2012; Van Oost et al., 2005a). These modelling approaches need to deal with modelling periods of at least decades to use SOC patterns for model testing and validating. Therefore, these models typically assume steady state erosion conditions and are driven by long-term erosion estimates either using Universal Soil Loss Equation (USLE; Wischmeier and Smith, 1960) technology (Dlugoß et al., 2012) or even more parsimonious approaches on global scales (Van Oost et al., 2007). However, the problem of these types of coupled models is that the event-based nature of erosion is statistically integrated into long-term mean annual erosion rates. This might be appropriate when focusing on bulk soil erosion alone, but the effects of the large temporal variability of erosion processes on C sequestration, mineralisation and lateral SOC export from a catchment remain unclear.

* Corresponding author at: Institut für Geographie der Universität Augsburg, Alter Postweg 118, D-86135 Augsburg, Germany.
E-mail address: peter.fiener@geo.uni-augsburg.de (F. P.).
[1] Equal contribution of both authors.

At least three effects might bias the model-based analysis of SOC redistribution induced C fluxes using long-term mean erosion rates as the driver in coupled models: (i) Spatial patterns of erosional and depositional areas vary depending on erosion event characteristics. (ii) On the one hand, pronounced erosion and deposition in some years might accelerate dynamic replacement at erosional sites, while on the other hand, burial of SOC might be more effective when large quantities of SOC are buried at once and hence are more effectively protected from mineralisation due to the decrease of SOC turnover with depth (e.g. Berhe and Kleber, 2013; Berhe et al., 2008; Rosenbloom et al., 2001). (iii) The potentially most important effect is the enrichment of C in delivered sediments compared to the parent soil material within the catchment that is not integrated in long-term models but which has been proven in many experimental studies (e.g. Schiettecatte et al., 2008b). In general, two event-size specific processes affect the C enrichment in delivered sediments. Plot experiments indicate that SOC is preferentially eroded and hence delivered sediments are enriched in carbon. Here enrichment ratios decline with increasing erosion, which is either expressed as sediment concentration in runoff (Wang et al., 2010, 2013) or as sediment delivery rate (Schiettecatte et al., 2008b). The observed decline in selectivity is associated to a shift from selective interrill erosion to more or less unselective rill erosion (Schiettecatte et al., 2008b). Other studies more generally focus on the enrichment of substances associated to fine particles on different scales (plot to small catchment) without explicitly analysing enrichment processes during single events. These studies also indicate a general decline of C or P (phosphorus) enrichment with increasing event or long-term erosion rates (Auerswald and Weigand, 1999; Menzel, 1980; Polyakov and Lal, 2004; Sharpley, 1985). The second important process affecting carbon enrichment in the sediment delivery of a catchment is the preferential deposition of coarse and heavy particles, while carbon is mostly associated to fine and light sediments (Schiettecatte et al., 2008a; Van Hemelryck et al., 2010a; Wang et al., 2010). For example, Wang et al. (2010) found a depletion ratio of SOC in deposits ranging from 0.50 to 0.91, with lowest values in the winter (i.e. highest SOC enrichment in delivered sediments due to preferential deposition of coarse and heavy particles not included in aggregates) and highest values in the summer when sediments are mostly transported as aggregates. Similar but somewhat more extreme depletion during deposition in a flume experiment was found by Van Hemelryck et al. (2010a) with depletion ratios ranging from 0.35 to 0.75.

As described above, it is very difficult to address all these potential effects resulting from the temporal variability of erosion processes, as their analysis calls for measured data with a very high temporal resolution (minutes to hours) of rainfall, dynamic soil properties (e.g. moisture), soil cover, management, runoff, sediment delivery, etc., and for a continuous long-term monitoring (decades) of C sequestration and mineralisation following different erosion events. To address all aspects at once and take short-term processes of soil and SOC redistribution as well as long-term effects on C mineralisation and sequestration into account calls for a modelling study that couples a high resolution, process-based, sediment-size selective erosion model (e.g. Fiener et al., 2008; Laflen et al., 1997; Schmidt et al., 1999) with a state-of-the art C turnover model (e.g. Coleman and Jenkinson, 2008; Skjemstad et al., 2004). However, these model types are highly data demanding (e.g. they need exact timing of tillage operations) and therefore an application on a time scale of decades or centuries is associated with large uncertainties as most input data need to be estimated from generally available data sources, e.g. average harvesting time for a region.

The main aim of this modelling study is to assess the importance of variability of event-driven soil erosion when analysing the long-term effects of SOC redistribution on C mineralisation and burial within an arable landscape. Instead of tackling the issue with a process-based model with its specific difficulties that were identified above, we conceptually integrated the most important processes into the well-established long-term erosion and C turnover model SPEROS-C (Van Oost et al., 2005b), which operates at timescales of several years to decennia and that had already been successfully implemented at the study site (Dlugoß et al., 2012). This means that the event-driven variability of annual erosion, based on high resolution erosivity data (5-min, 50 years), an erosion magnitude specific SOC enrichment in delivered sediments, and depletion ratios based on different approaches and literature data were integrated into SPEROS-C.

2. Methods

2.1. Combined soil redistribution and SOC dynamics modelling

The model SPEROS-C (Dlugoß et al., 2012; Nadeu et al., 2015; Van Oost et al., 2005a) combines the water and tillage erosion model WaTEM (Van Oost et al., 2005a) with the Introductory Carbon Balance Model (ICBM; Andrén and Kätterer, 1997). The original model code was recently restructured and transferred from Delphi (Borland, USA) to Lazarus, which is a Delphi compatible cross-platform IDE for Free Pascal (http://www.lazarus.freepascal.org). The modifications made to the model for this study are described in detail here, while the original structure and process descriptions are only summarized. A detailed description of SPEROS-C can be found in Van Oost et al. (2005b) and Dlugoß et al. (2012).

In general, SPEROS-C is a raster-based, spatially explicit, multiple soil layer model that calculates soil and associated SOC redistribution by water, tillage and harvest erosion in an annual time step. The water erosion component is based on (i) the assessment of the potential erosion rate for each grid cell, (ii) the assessment of the local transport capacity, and (iii) a topography-based routing algorithm that redistributes the produced sediment over the land surface by accounting for flow-direction and the spatial pattern of the transport capacity. The potential water erosion for each grid cell is calculated according to the Revised Universal Soil Loss Equation (RUSLE), while the local transport capacity TC (kg m^{-1} a^{-1}; Eq. (1)) is assumed to be proportional to the erosion potential:

$$TC = ktc \cdot R \cdot C \cdot P \cdot K \cdot LS \tag{1}$$

where ktc is the transport capacity coefficient, R, C, P, K, L and S are the RUSLE (Renard et al., 1996) factors: R is the rainfall erosivity factor, C is the cover management factor, P is the conservation practice factor, K the soil erodibility factor, L the slope length factor, and S the slope gradient factor.

Erosion and deposition caused by tillage is calculated following the diffusion-type approach developed by Govers et al. (1994), while soil loss due to crop harvesting (Ruysschaert et al., 2004, 2005) can be included for root crops.

The ICBM (Andrén and Kätterer, 1997) describes SOC dynamics using two SOC pools ("young" and "old") and four C fluxes (C input from plants, mineralisation from the young and the old pool, and humification). In SPEROS-C, the C input into the soil by plant residues is estimated as a ratio of crop yield and added to the plough layer, while the C input by roots is assumed to decrease with soil depth following an exponential root density function. Additionally, the C input by cover crops and/or organic manure can be specified for the plough layer.

SOC erosion (C_{ero}) from the topsoil layer for the two SOC pools is modelled for each time step using the results from soil redistribution by water, by tillage, and the soil loss due to root crop harvesting. It is calculated as

$$C_{ero} = SOC_1 \cdot M_{ero}/M_1 \tag{2}$$

with SOC_1 being the amount of SOC in the first soil layer (g), M_{ero} being the mass of eroded soil (g) and M_1 being the total mass of the first soil layer (g).

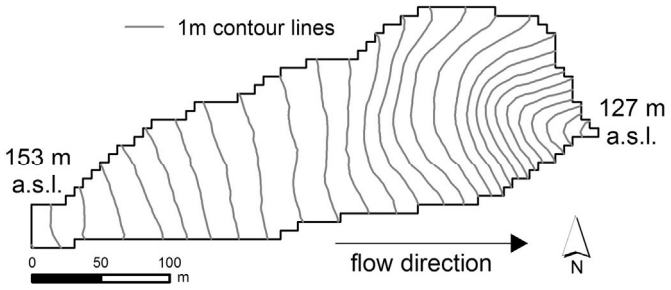

Fig. 1. Topography and flow direction of the study site.

SPEROS-C characterises the soil profile up to 1 m in depth. In order to assess the role of event-size more accurately, we refined the vertical representation of the SOC profile for this study: The 1 m soil profile is discretised in 10 layers of 0.1 m depth each. In order to reflect the plough layer, carbon input and decomposition are assumed to be homogeneous for the upper 0.2 m of the soil profile. The SOC profile is updated once a year to account for the vertical advection of SOC in response to erosion or deposition. After updating the profile, the ICBM model is applied to simulate carbon input and decomposition for each time step.

2.2. Model implementation

2.2.1. Study site and parameterisation

To implement the model in a realistic set-up, we used measured data as model input. However, as our intention was not to reproduce a specific situation in a specific catchment, but to analyse system behaviour that has not yet been measured with a high temporal resolution over a time period of decades, we combined input data of different regions resulting in a virtual catchment approach.

Most of the basic input data (e.g. catchment area, topography, land use and management) were taken from a small catchment (4.2 ha) located in the Pleiser Hügelland, a hilly landscape about 30 km southeast of Cologne in North Rhine-Westphalia, Germany (altitude 125–154 m above sea level; slopes from 1° to 9°; 50°43′N, 7°12′E) (Fig. 1). Due to the fertile, silty and silty-loamy soils (mean sand, silt and clay content of 13%, 68% and 19%, respectively) classified as Luvisols (FAO, 1998), which originated from loess deposits, and the proximity of the region to the cities of Bonn and Cologne, the test site has a long history of arable land use (Preston, 2001). Today, the site is intensively used for arable agriculture. Since the 1950s the crop rotation has consisted of winter wheat (*Triticum aestivum* L.), winter barley (*Hordeum vulgare* L.), and sugar beet (*Beta vulgaris* L.). Starting in the early 1980s, soil conservation has become more important and mustard (*Sinapis arvensis* L.) has been cultivated as a cover crop after winter barley while tillage intensity has been reduced. An analysis of detailed SOC maps of three soil depths (0–0.25 m; 0.25–0.50 m; 0.50–0.90 m, respectively) based on a sampling raster of 17.7 by 17.7 m showed the importance of soil redistribution for SOC patterns (Dlugoß et al., 2010). Based on these data, SPEROS-C was already applied in the catchment (Dlugoß et al., 2012) and hence model parameters could be taken from this study. Site-specific mineralisation rates of the two C pools were calibrated by an inverse modelling approach using SOC data from 65 soil profiles within the study site showing neither erosion nor deposition (Dlugoß et al., 2012). The transport capacity coefficient was set to 50 m by iteratively comparing the modelled total deposition rate at two validation points to deposition rates derived from accelerated mass spectrometry ^{14}C data (Dlugoß et al., 2012) at these points. The simulation period was set from 1951, when arable agriculture in the region was intensified, to 2007, when SOC inventory measurements were carried out (Dlugoß et al., 2010) and used for model validation (Dlugoß et al., 2012). However for this study, we used a simplified and constant crop rotation under conventional tillage of winter wheat, winter barley, and sugar beet for our virtual catchment. An increased mineralisation of SOC during transport by water was no longer considered in this study, since this effect was shown to be negligible in several experimental studies on silty–loamy soils (e.g. Bremenfeld et al., 2013).

2.2.2. Temporal variability of soil erosion

As no long-term, high-resolution rainfall data (5–10 min time step), which are necessary to account for the effects of single events on annual rainfall erosivity, are available for the entire simulation period in the catchment, we used data from a meteorological station located in the central Ruhr area about 80 km to the north of the study site (temporal resolution ≤ 5 min, data available 1937–2007). These data were extensively tested for consistency in an earlier study (Fiener et al., 2013), and generally are well suited to represent the potential variability of rainfall erosivity in central Europe (Fiener et al., 2013). The high resolution precipitation data made it possible to derive daily rainfall erosivity (daily USLE *R* factors), which is highly variable throughout the simulation period (Fig. 2). The daily rainfall erosivity was used to calculate yearly varying *R* factors and in combination with daily soil cover data, it was also used to calculate yearly varying USLE *C* factors. The combined variability of annual $R \cdot C$ for the simulation period is given in Fig. 3.

In order to consider different realisations of frequency and magnitude of erosive events, a set of 100 randomly sampled 57 year sequences of *R* and *C* factors was created as model input. Therefore, the years with their specific daily *R* factor distribution (Fig. 2) were sampled with replacement. While the original crop rotation was maintained, these new sequences of daily *R* factors were used to calculate 100 representations of yearly varying *R* and *C* factors representing different frequency and magnitude of erosive events within different years. As the sampling was done with replacement, the same *R* and *C* factor values can occur several times in the new sequences. The random arrangement also eliminated a positive temporal trend in erosivity that was found in the original data (Fiener et al., 2013).

2.2.3. Selectivity of soil erosion and deposition

To include a potential erosion magnitude-specific enrichment of SOC due to the preferential erosion of fine and light particles by interrill erosion, we implemented an enrichment equation (Eq. (3)) to calculate the raster cell-specific SOC enrichment ratio *ER* (dimensionless) for every raster cell with net erosion depending on its annual water erosion rate

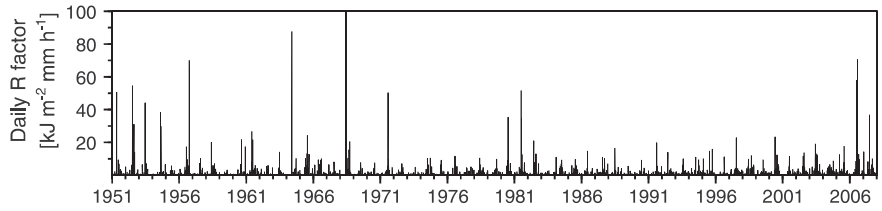

Fig. 2. Daily rainfall erosivity (USLE *R* factor) [kJ m^{-2} mm h^{-1}] for the simulation period 1951 to 2007 derived from 5-min precipitation data from a precipitation gauge in the central Ruhr area.

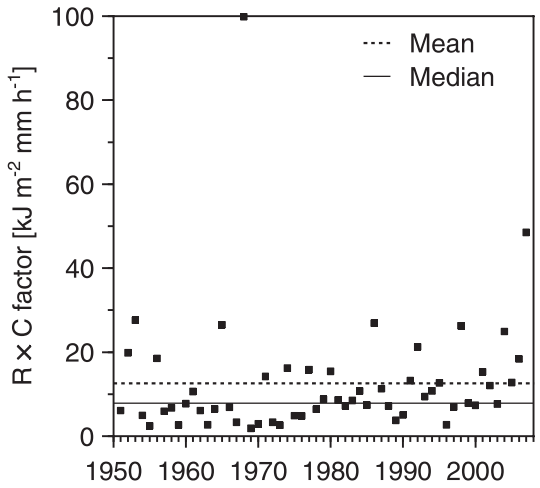

Fig. 3. Time series of annual erosivity (USLE *R* factor [kJ m^{-2} mm h^{-1}]) calculated from 5-min precipitation multiplied by the annual management factor (USLE *C* factor [—]) derived from daily erosivity and daily soil cover used as model input; 5-min precipitation data were taken from a precipitation gauge in the central Ruhr area, while soil cover was derived for the study site south-east of Cologne.

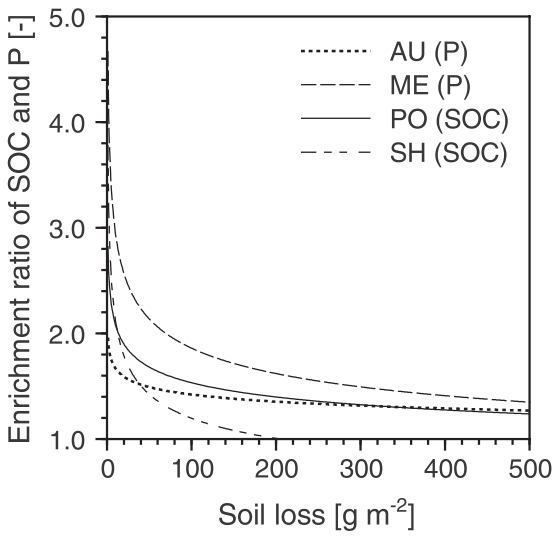

Fig. 4. Enrichment ratios of SOC and P during erosion processes derived from measurements on different scales by Auerswald and Weigand (1999) (AU), Menzel (1980) (ME), Polyakov and Lal (2004) (PO), and Sharpley (1985) (SH).

SE (g m^{-2}):

$$ER = \alpha \cdot SE^{-\beta} \quad (3)$$

with α and β as dimensionless empirical parameters.

This type of negative power function was used in several process studies representing erosion magnitude either as sediment concentration in measured runoff (Wang et al., 2010) or as sediment delivery rate (Schiettecatte et al., 2008b). However, it was also derived from more general relations between erosion rates on different spatio-temporal scales and their specific enrichment ratios (Polyakov and Lal, 2004). As SPEROS-C calculates raster cell-specific erosion rates but does not address runoff dynamics, we used the later type of relation as given in Auerswald and Weigand (1999), Menzel (1980), Polyakov and Lal (2004) and Sharpley (1985), which resulted in different values for α and β (Table 1). The different parameter sets to calculate SOC enrichment were used to represent a wide range of possible soil textures, spatial scales and erosion event magnitudes (Table 1). Unfortunately, direct measurements of SOC enrichment are mostly based on plot experiments (e.g. Polyakov and Lal, 2004; Sharpley, 1985). Therefore we added two enrichment parameter sets originally derived from the enrichment of phosphorus (Auerswald and Weigand, 1999; Menzel, 1980), which represent a much wider range of soil textures (sandy loam to silty loam), spatial scales (plots to small catchments) and erosion event magnitudes (0.3 to 25 000 kg ha^{-1}) (Table 1). The transfer of parameter sets derived from P enrichment to the enrichment of SOC is based on the conservative assumption that P and C are mostly associated to fine particles and that effects of the smaller density of C can be ignored. This simplification seems to be reasonable due to the similarity of the different enrichment functions for C and P (Fig. 4). Since this study intends to evaluate the potential effects of SOC enrichment under different environmental conditions and not to reproduce the behaviour of a specific catchment, our enrichment parameters should reasonably represent a potential spectrum of results. To introduce the process of selective deposition that leads to a depletion of C in deposits, we used a range of depletion ratios *DR* from literature (Van Hemelryck et al., 2010a; Wang et al., 2010) (Table 2).

Enrichment due to (interrill) erosion is integrated into SPEROS-C by multiplying the delivered SOC from each raster cell that experiences net erosion with an event-size specific enrichment ratio following Eq. (3). Enrichment due to deposition is calculated based on a depletion ratio applied at depositional sites. This carbon is not deposited but is added to the carbon routed over areas of net deposition. This approach is not linked to event size, as to our knowledge there is no approach available that allows conceptually linking C depletion ratios to bulk soil deposition without taking e.g. event and location specific runoff depths into account.

2.2.4. Model scenarios

Overall, the following model runs were performed to evaluate the effects of annual erosion variability and SOC enrichment in delivered sediment on lateral and vertical SOC fluxes (overview in Table 2): Run 1 represents long-term mean erosion (n = 57) without (event-specific) enrichment of SOC due to selective erosion or deposition. For this run, a mean *R* and *C* factor for the overall simulation period of 57 years was used as model input. This model run represents the typical coupled erosion and C turnover modelling for long time periods as performed in earlier studies (Dlugoß et al., 2012; Van Oost et al., 2005a). Subsequently this run is referred to as the reference.

Table 1
Parameters and experimental side conditions from different studies (Auerswald and Weigand, 1999, AU; Menzel, 1980, ME; Polyakov and Lal, 2004, PO; Sharpley, 1985, SH) that were used to calculate the SOC enrichment ratio *ER* at erosional sites based on Eq. (3).

Reference		Soil texture	Spatial scale	No. of events	Erosion [kg ha^{-1}]	Enrichment Phosphorus (P); soil organic carbon (SOC)	Parameters derived to calculate *ER* (see Eq. (3))	
							α	β
Auerswald and Weigand(1999)	AU	Sandy to silty loam	Plot to small catchment	210	1 to 3000	P	1.96	−0.07
Menzel(1980)	ME	Sandy to silty loam	Plot to small catchment	952	0.3 to 25,000	P	4.67	−0.20
Polyakov and Lal(2004)	PO	Silty loam	Plot	12	34 to 1307	SOC	2.83	−0.13
Sharpley(1985)	SH	Loam	Plot	16	10 to 620	SOC	3.78	−0.25

Table 2
Summary of modelled scenarios and parameters used; see Table 1 for details regarding enrichment ratios.

ID	USLE *R* and *C* factors	Number of model runs	Enrichment ratio *ER* at erosional sites			Depletion ratio *DR* at depositional sites
			α in Eq. (3)	β in Eq. (3)	Reference	
1	Mean n = 57 years	1	–	–	–	–
2–101	Yearly varying	100	–	–	–	–
102–201	Yearly varying	100	1.96	−0.07	AU	–
202–301	Yearly varying	100	4.67	−0.20	ME	–
302–401	Yearly varying	100	2.83	−0.13	PO	–
402–501	Yearly varying	100	3.78	−0.25	SH	–
502–601	Yearly varying	100	–	–	–	0.35
602–701	Yearly varying	100	–	–	–	0.63
702–801	Yearly varying	100	–	–	–	0.91
802–901	Yearly varying	100	1.96	−0.07	AU	0.63

Runs 2–101 represent annual erosion variability without (event-specific) enrichment due to selective erosion or deposition. These 100 runs were performed with the randomly arranged annual *R* and *C* factors as model input as described above. Subsequently, these runs are referred to as variable erosion.

Runs 102–501 represent variable erosion with erosion magnitude specific enrichment of SOC due to selective interrill erosion. Variability of *R* and *C* factors equals the variable erosion runs, while SOC enrichment at erosion sites is calculated based on the different parameterisation of Eq. (3) (Table 2), resulting in 400 runs, subsequently referred to as variable erosion and enrichment.

Runs 502–801 represent variable erosion with enrichment due to selective deposition. Variability of the *R* and *C* factors equals the variable erosion runs, while SOC depletion at depositional sites is calculated by applying three depletion ratios (0.35, 0.63, and 0.91) derived from Wang et al. (2010) and Van Hemelryck et al. (2010a) resulting in 300 runs, subsequently referred to as variable erosion and depletion.

To analyse the combined effect, runs 802–901 represent variable erosion with enrichment due to selective erosion and selective deposition. The parameters of Auerswald and Weigand (1999) are exemplarily used in the enrichment equation (Eq. (3)) as their parameter-set is based upon a wide range of soil textures, spatial scales and event sizes but is less extreme compared to the even larger data set of Menzel (1980). The depletion ratio was set to the average value of 0.63. This results in 100 runs, subsequently referred to as variable erosion with enrichment and depletion.

3. Results

3.1. Effects of erosion variability and SOC enrichment on C fluxes in single years

Using one exemplary time series of *R* and *C* factors as model input (one example out of runs 2–101), allows focusing on the effects of erosion variability and erosion magnitude specific enrichment in single years compared to the reference (run 1) (Fig. 5). The reference shows an underestimation of the C sink due to dynamic replacement at erosion sites caused by reduced SOC mineralization following the lateral removal of SOC and by the continued C input by plants on arable land (Harden et al., 1999; Stallard, 1998) in extreme erosive years (e.g. 1968, 2007) and an overestimation in low erosive years (e.g. around 1960) compared to variable erosion (Fig. 5A). Additionally, only including enrichment due to (interrill) erosion (corresponding runs out of 102–501) makes the C uptake due to dynamic replacement at erosion sites in each year greater than without enrichment, since more SOC is laterally removed, which could subsequently be dynamically replaced. No substantial changes in the vertical C fluxes at erosion sites can be observed when only integrating different depletion ratios at depositional sites (corresponding runs out of 502–801). This is also true when looking at the corresponding combined model run (one out of runs 802–901), which at erosional sites resembles the results from only integrating enrichment following Auerswald and Weigand (1999).

At depositional sites, the reference underestimates the erosion induced C mineralization compared to single high erosive years (e.g. 1968, 2007) and overestimates these fluxes compared to low erosive years (e.g. around 1960; Fig. 5B). For the catchment scale integrated vertical C flux, i.e., the weighted spatial mean of the C sink at erosional sites and the C source at depositional sites (data not shown), both effects only partly compensate the under- and overestimation of dynamic replacement at erosional sites. This is due to the fact that depositional sites only cover a small part of the catchment (~19% of the catchment area) and hence even in case of pronounced mineralization at depositional sites, this does not level out dynamic replacement at erosional sites. Adding enrichment of SOC due to erosion results in a substantially higher mineralization at depositional sites compared to the runs without enrichment, since the deposited material contains more SOC compared to the deposited material without enrichment. The modelled enrichment effect varies depending on the parameterisation of Eq. (3) with the largest effect obtained using the parameterisation from Menzel (1980) and the least pronounced effect using the parameterisation from Auerswald and Weigand (1999). A contrary behaviour can be found if only depletion at depositional areas is implemented. Depending on the depletion ratio, depositional areas may become a net C sink (Fig. 5B). Combining SOC enrichment due to erosional processes and depletion via depositional processes results in a reduced C source from deposits than those modelled for the variable erosion runs with enrichment alone (Fig. 5B) since both processes partly compensate each other.

The temporal development of lateral SOC export for variable erosion corresponds to the time series of high and low erosive years, while for mean annual erosion there is only a small annual variability resulting from the implemented crop rotation (Fig. 5C). Overall there is a tendency that variable erosion produces a slightly lower C export. Including enrichment due to erosion processes stresses the importance of low erosive years with high enrichment ratios. In low erosive years (e.g. 1963 in the shown example) the relative increase of lateral SOC export is higher than for high erosive years (e.g. 1968 in the shown example) compared to variable erosion alone (Fig. 5C). In contrast, the lateral C export is increased by the same magnitude for low and high erosive events compared to variable erosion alone when implementing C depletion at depositional sites (Fig. 5C). It is interesting to note that for the vertical C fluxes at depositional sites enrichment and depletion may compensate each other (Fig. 5B), while for the lateral C export from the catchment they may amplify each other in the combined model run.

The overall C balance for the catchment, that is calculated as the weighted spatial mean of the vertical C fluxes at erosion and deposition sites plus the lateral C export, turns from being negative into positive with ongoing soil erosion for most of the model runs (Fig. 5D). This can be explained by the fact that the simulations start assuming a spatially uniform SOC value at steady state, since no data of the initial SOC distribution are available. Hence, with each year of ongoing lateral SOC redistribution, the system moves away from equilibrium between C

inputs and outputs. Especially at erosional sites, dynamic replacement of C constantly increases, as a new equilibrium is not reached under erosional conditions within the simulation period. When this C sink function is not offset via export and additional mineralization at depositional sites, the system slowly moves to a stronger C sink. Comparing the reference with the variable erosion, an expected higher variability in the yearly balance is shown when using variable *R* and *C* factors as input. However, the variability of the C balance is smaller than that of the lateral SOC export (Fig. 5C). In extreme erosive years, large SOC exports are buffered by high rates of dynamic replacement (Fig. 5A). When including enrichment due to erosion processes, the C balance (Fig. 5D) is always lower than the balance without enrichment, i.e., more C is lost in those years with a generally negative C balance and the C sink is lower or even turns into a C source in those years when the C balance is generally positive. Implementing depletion due to selective deposition results in a similar effect. Combining erosional enrichment and depositional depletion increases C effluxes from deposits and the lateral SOC export from the catchment. Hence, the combination of both processes weakens the potential C sink or increases the potential source function of the catchment.

3.2. Cumulative effects over the simulation period

Cumulating the C fluxes at erosional and depositional areas (Fig. 6A,B) over the entire modelling period generally reveals the same behaviour of the C fluxes as shown in Fig. 5A, B with a C sink at erosional areas and a C source at depositional areas of roughly half the size. The cumulative C fluxes from the reference (run 1) resemble the resulting mean cumulative C flux from the 100 variable erosion runs (runs 2–101). However, the 100 representations of different frequency and magnitude of erosive events result in a distinct variability of cumulative vertical C fluxes at the end of the simulation period ranging between a C sink of 88 g C m^{-2} and 122 g C m^{-2} at erosional areas and a C source between −51 g C m^{-2} and −72 g C m^{-2} at depositional areas, respectively. This variability increases with ongoing soil erosion, and hence the reference would increase to deviate e.g. from the most extreme C source at depositional sites in form of an underestimation and from the lowest C source in form of an overestimation in a prolonged simulation period.

The results further indicate that the mean of the variable erosion runs leads to a slightly smaller SOC export (Fig. 6C) that results in an overall smaller cumulative C loss. However, it is obvious that the mean SOC export is highly uncertain as indicated by the 100 variable erosion runs. For the overall erosion induced cumulative C balance (Fig. 6D), our modelling study indicates that (i) variable erosion also results in a substantial variability of cumulative fluxes at the end of the simulation period (ranging from a C source of −14 g C m^{-2} to a C sink of 9 g C m^{-2} for the 100 different representations), (ii) erosion leads to an increasing negative C balance at the beginning of the simulation period due to the loss of carbon via lateral C export but leads to a less pronounced C source or even a C sink from the 1980s onwards, since increasing dynamic replacement offsets the lateral C loss from the catchment and vertical C loss due to mineralization at depositional sites, and (iii) this trend might be underestimated in the reference compared to specific representations of frequency and magnitude of erosive events. With ongoing soil erosion, the cumulative C balance resulting from the reference and the variable erosion runs diverge continuously and hence constitute substantially different results. As long as the system does not reach a new equilibrium, which is not the case for the simulation period, this effect will even be enlarged for longer simulation periods.

Additionally implementing different enrichment ratios due to selective erosion in the variable erosion runs (runs 102–501) even increases the variability of cumulative vertical C fluxes at erosional and depositional sites at the end of the simulation period. C fluxes range from 125 to 274 g C m^{-2} at erosional sites and from −446 to −142 g C m^{-2} at depositional sites (Fig. 7A, B). These wide ranges indicate the sensitivity

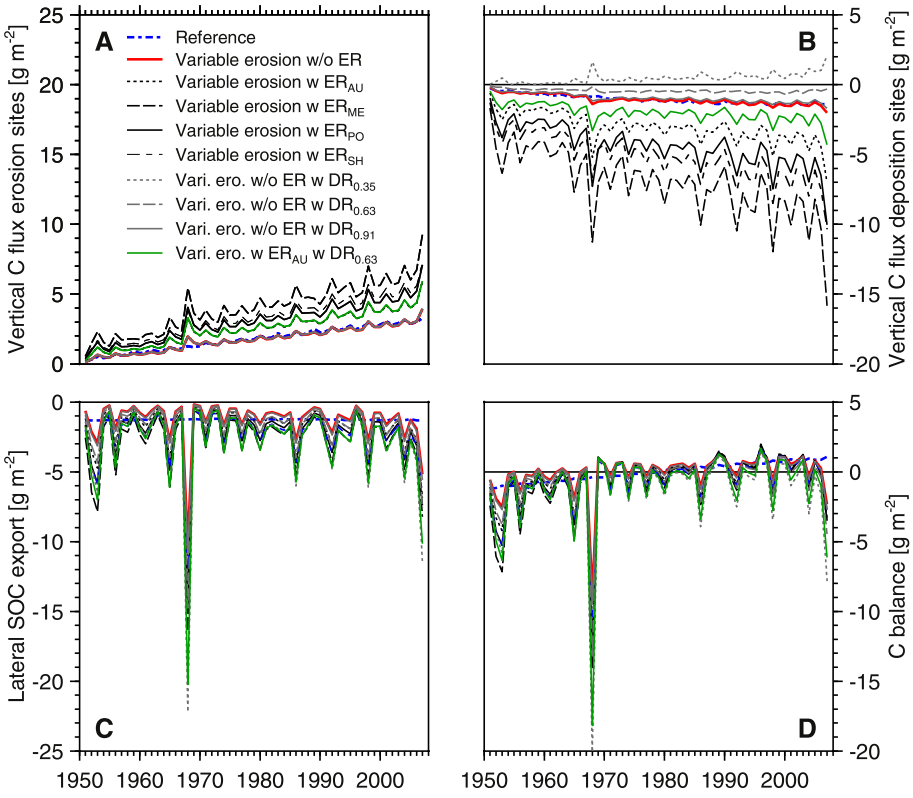

Fig. 5. Modelled erosion induced C fluxes for the reference run (run 1), one exemplary variable erosion run (one out of runs 2–101), four runs with selective erosion ($ER_{AU\text{-}SH}$, corresponding runs out of 102–501), three runs with selective deposition ($DR_{0.35–0.91}$, corresponding runs out of 502–801), and one combined run (ER_{AU} plus $DR_{0.63}$, corresponding runs out of 802–901); see Table 2 for details regarding abbreviations and model runs. (All figures are given in colour in the web version of this article.)

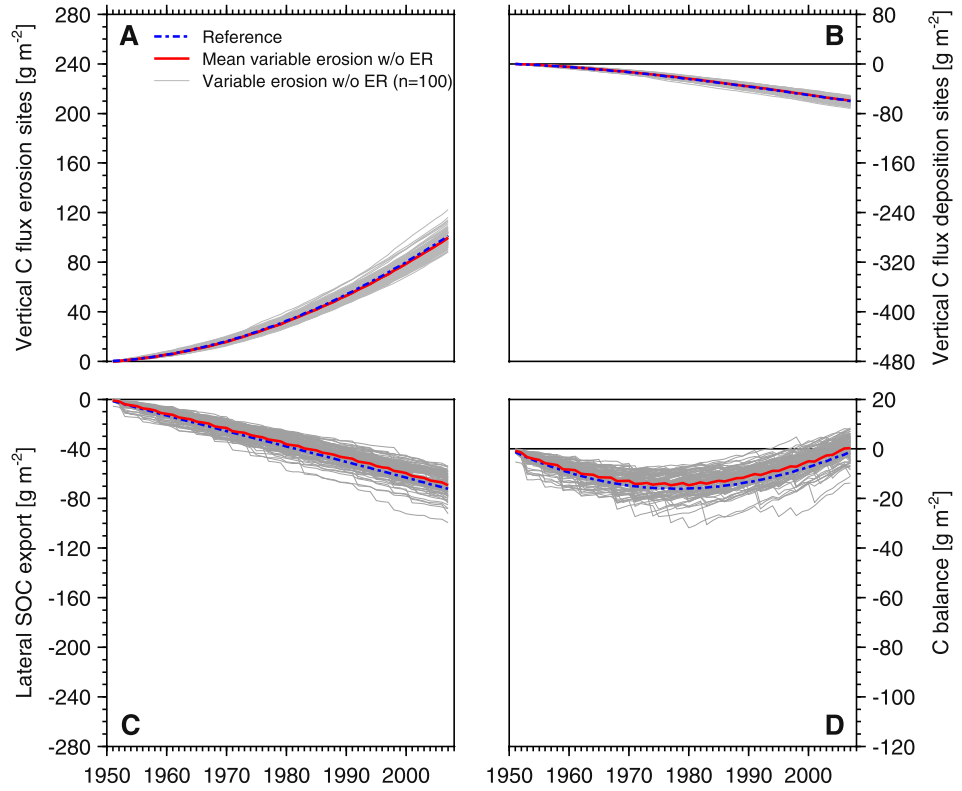

Fig. 6. Modelled cumulative erosion induced C fluxes taking neither enrichment at erosional sites nor depletion at depositional sites into account; reference without variable erosion (run 1), variable erosion (runs 2–101) and mean variable erosion (mean out of runs 2–101); see Table 2 for details regarding abbreviations and model runs.

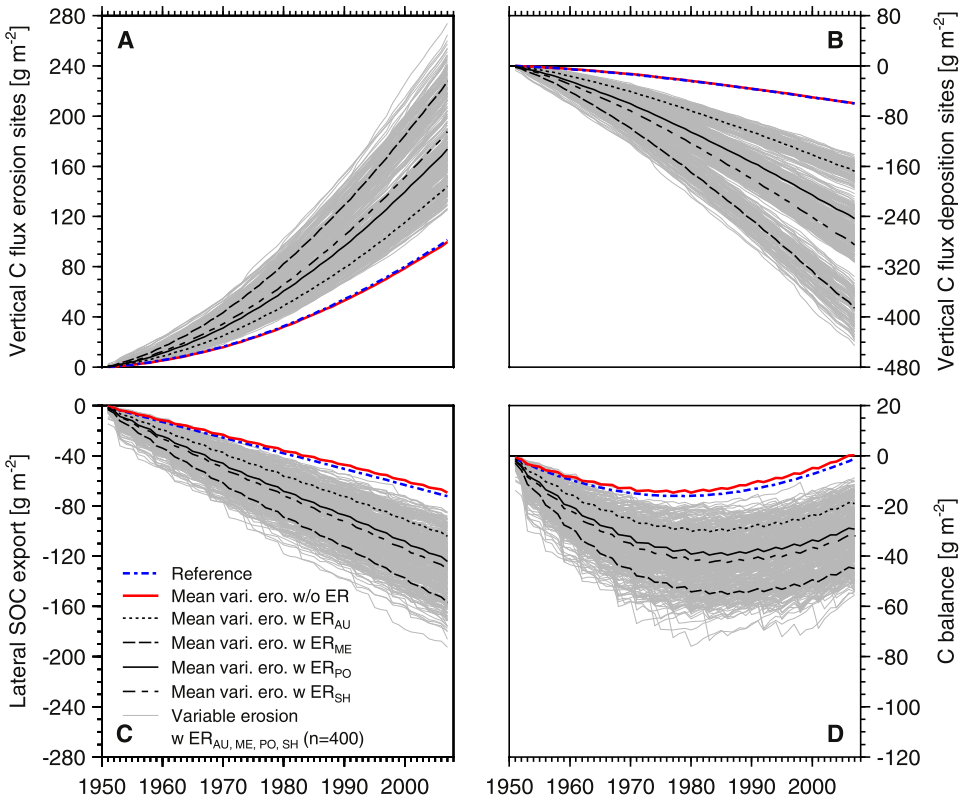

Fig. 7. Modelled cumulative erosion induced C fluxes illustrating different enrichment ratios *ER* due to erosion; reference without variable erosion (run 1), mean variable erosion (mean out of runs 2–101), variable erosion with different enrichment approaches ($ER_{AU\text{-}SH}$, runs 102–201, 202–301, 302–401, and 402–501, resp.), and the means of the variable erosion with different enrichment approaches are shown; see Table 2 for details regarding abbreviations and model runs.

of the modelled C fluxes on the implemented enrichment approach. At depositional sites this effect is most pronounced when using enrichment by Menzel (1980). Here on average, 320 g C m^{-2} are additionally mineralized within the modelling period compared to the mean without enrichment. For the cumulative lateral SOC export, again the variability of the single variable runs is increased when including enrichment (Fig. 7C) compared to the runs with variable erosion alone (Fig. 6C) at the end of the simulation period. All representations of variable erosion with enrichment (Fig. 7C) constitute a higher lateral SOC loss for the simulation period than the reference with a range from −85 g C m^{-2} to −193 g C m^{-2}. The cumulative C balances (Fig. 7D) all indicate that the system under consideration, i.e. a first-order catchment, loses C when enrichment of erosion processes is taken into account.

When including only depletion of SOC due to depositional processes for variable erosion (runs 502–801), the depositional sites switch from a relative strong C source (C source of reference of −60 g C m^{-2}) into a weaker C source or even into a small C sink (maximum C sink of 44 g C m^{-2}, Fig. 8B) for the most extreme depletion ratio. Including depletion also promotes lateral SOC delivery from the catchment (Fig. 8C), which is in the same order of magnitude for the highest modelled depletion effect (maximum SOC export in 2007 = −120 g C m^{-2} for $DR = 0.35$) as the mean effect when including enrichment at erosional sites (mean maximum SOC export from AU, ME, PO, SH = −109 g C m^{-2}; Figs. 7C vs. 8C). The overall range of the cumulative C balances (Fig. 8D) at the end of the simulation period lies between a C sink of 5 g C m^{-2} and a C source of −112 g C m^{-2} depending on the assumed depletion ratio and the representation of frequency and magnitude of water erosion.

Exemplarily combining all analysed processes (variable erosion, enrichment and depletion) by using the enrichment ratio according to Auerswald and Weigand (1999) and a depletion ratio of 0.63 (runs 802–901) shows that some processes potentially compensate each other, while others can amplify the C fluxes (Fig. 9). Vertical C fluxes at erosional sites (Fig. 9A) are in the same order of magnitude as for model runs 102–201 (Fig. 7A). However, there are large deviations in vertical C fluxes from depositional sites (Fig. 9B). While variable erosion with enrichment (runs 102–201) moves the depositional sites to a relatively strong C source (mean of −167 g m^{-2} in 57 years (n = 100)), the modelled depletion effect alone (runs 602–701) results in a C source of roughly 14% of that size (mean of −24 m^{-2} in 57 years (n = 100)). Combing enrichment and depletion, at least with this model parameterisation, leads to a C source of 110 g C m^{-2} (Fig. 9B). While enrichment and depletion effects upon C fluxes at depositional sites level out, both processes amplify lateral SOC delivery from the catchment (Fig. 9C) by adding ~50% exported C compared to the means resulting from runs 102–201 and 602–701. Looking at the C balance (Fig. 9D), the most pronounced effect could be found when C enrichment and depletion processes are combined (mean of −58 g C m^{-2} in 57 years (n = 100)).

4. Discussion

In general, our modelling study indicates that ignoring the episodic character of water erosion processes and the erosion magnitude specific SOC enrichment due to erosion and the SOC depletion at deposits may lead to a substantial misinterpretation of erosion-induced C fluxes. With respect to erosion variability alone (runs 2–101), the differences between the mean C fluxes of the 100 variable runs and the reference run using a mean erosion rate are small to negligible (Fig. 10). Nevertheless, ignoring this variability makes interpreting measured SOC patterns in the context of erosion patterns (e.g. Dlugoß et al., 2010; Meersmans et al., 2011) difficult due to the large variability that is inherent in the single representations of the 100 runs with differing frequency and magnitude of erosion. However, it is worth emphasizing that SPEROS-C only indirectly accounts for erosion variability, i.e., when combining

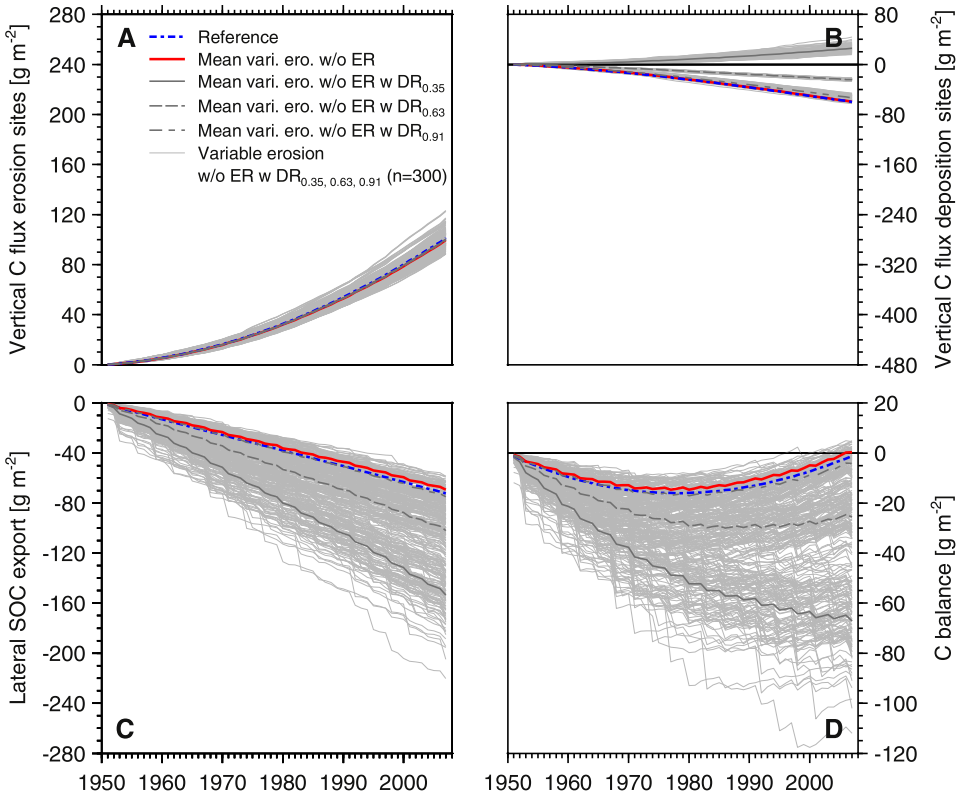

Fig. 8. Modelled cumulative erosion induced C fluxes illustrating different depletion ratios *DR* at depositional sites; reference without variable erosion (run 1), mean variable erosion (mean out of runs 2–101), variable erosion with different depletion ratios ($DR_{0.35–0.91}$, runs 502–601, 602–701, and 702–801, resp.), and the means of the variable erosion with different depletion ratios are shown; see Table 2 for details regarding abbreviations and model runs.

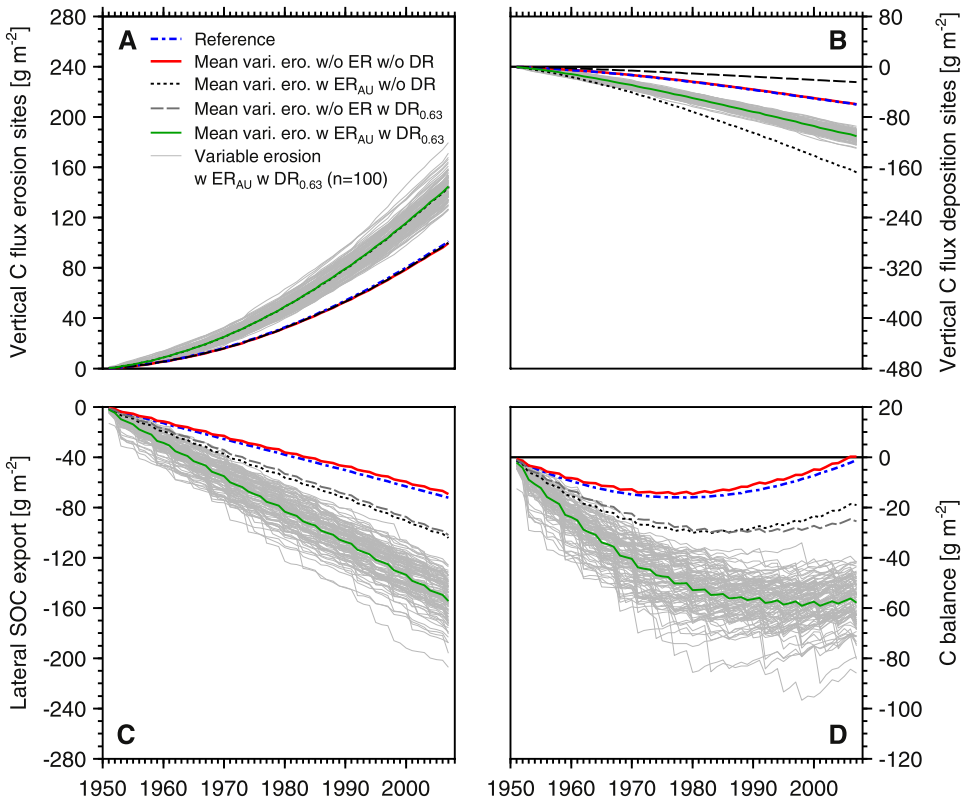

Fig. 9. Modelled cumulative erosion induced C fluxes illustrating the combined effect of enrichment at erosional and depletion at depositional sites; reference without variable erosion (run 1), mean variable erosion (mean out of runs 2–101), mean variable erosion with exemplary enrichment (ER_{AU}, mean out of runs 102–201), mean variable erosion with exemplary depletion ($DR_{0.63}$, mean out of runs 602–701), variable erosion with exemplary enrichment and depletion (ER_{AU} plus $DR_{0.63}$, runs 802–901) and its mean; see Table 2 for details regarding abbreviations and model runs.

event-based erosivity and daily crop cover into annual *R* and *C* factors. The effect of single very extreme events, which often dominate long-term erosion (Fiener and Auerswald, 2007; Nearing et al., 1999), is only taken into account in so far as these extreme events disproportionately affect the *R* and *C* factors. Nevertheless, the effect of such extreme events will be dampened, if the rest of the year is dominated by small erosive events. The yearly averaging will therefore lead to a conservative estimate of the effects of erosion variability on the erosion-induced C fluxes. Moreover, direct effects on CO_2 effluxes during or shortly after events (Bremenfeld et al., 2013; Van Hemelryck et al., 2010a) are ignored in SPEROS-C, which may partly balance the additional C sink function from erosion variability. Especially at depositional sites, increasing CO_2 effluxes were observed after large erosion events (Bremenfeld et al., 2013; Hu and Kuhn, 2014; Van Hemelryck et al., 2010a).

Including enrichment due to (interrill) erosion in the model runs with variable erosion (runs 102–501) results in a much more pronounced effect upon C fluxes with an even larger variability (Fig. 10). In general, the erosion event-size specific enrichment of SOC in delivered sediment is consistent with studies experimentally evaluating this process (Kuhn et al., 2010; Polyakov and Lal, 2004; Schiettecatte et al., 2008b), but our modelling study can only show potential effects of enrichment by using different parameterisations of Eq. (3). However, there is a substantial lack in knowledge in how to parameterise such an equation in a real catchment instead of a virtual one.

The depletion of carbon due to selective deposition has also been shown in experimental studies (e.g. Van Hemelryck et al., 2010a) and is consistent with results from sediment size-specific modelling approaches indicating that coarse particles are preferentially settled (e.g. Fiener et al., 2008) while smaller particles or micro-aggregates (clay and silt fraction) tend to show higher C concentrations (e.g. Virto et al., 2008). In our modelling study, depletion is implemented using three different depletion ratios found in literature (Van Hemelryck et al., 2010a; Wang et al., 2010) (runs 502–801), which is even a simpler approach than using an erosion rate specific enrichment ratio for erosional sites. Depending on the depletion ratio, the effect on the overall C balance can be even larger than the effect of SOC enrichment due to selective erosion (Fig. 10D). The approach used allows illustrating the interactions between SOC enrichment due to erosion processes and SOC depletion due to depositional processes. Combining both processes on the one hand dampens the vertical C losses from depositional sites (Fig. 10B) but on the other hand accelerates the overall C loss from the catchment (Fig. 10D). Hence, taking the combined effect of both processes into account, improves potential analyses of spatial SOC patterns in the context of soil redistribution patterns (e.g. Dlugoß et al., 2010).

The empirical enrichment and depletion ratios that we implemented in SPEROS-C are somewhat crude as they neither directly account for the processes during interrill erosion that lead to either total SOC (Kuhn et al., 2010) or SOC fraction-specific enrichment (Wang et al., 2013), nor do they directly account for the particle size-specific processes of deposition and re-entrainment (Hairsine et al., 2002) that lead to SOC fraction-specific deposition (Hu and Kuhn, 2014). However, more complex modelling approaches with focus on event-based particle-size selective erosion (e.g. Fiener et al., 2008; Laflen et al., 1997; Schmidt et al., 1999), which can more physically account for enrichment processes, cannot be fed with appropriate data for a period of more than 50 years. Hence, our approach can be seen as a first attempt to address long-term effects of SOC enrichment during single erosive events on estimates of erosion-induced C fluxes and their associated uncertainties. This seems to be especially important when long-term SOC burial and mineralisation at depositional sites (Fig. 10B) are to be evaluated,

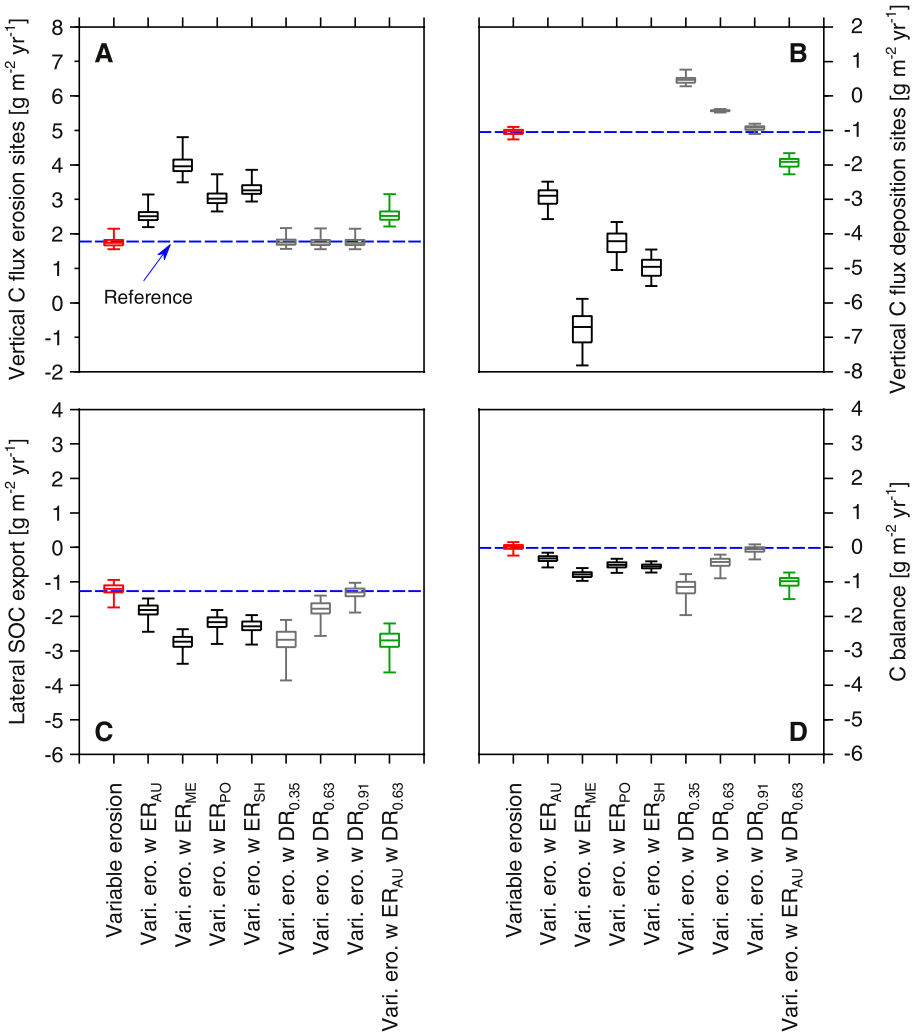

Fig. 10. Mean modelled erosion induced C fluxes for the simulation period 1951 to 2007; box–whiskers represent the median, 1st and 3rd quartiles, and minimum and maximum values calculated out of 100 model runs per category; the dashed line represents the reference model run (run 1); see Table 2 for details regarding abbreviations and model runs.

which commonly is analysed based on deposition depths at colluvial and alluvial sites without taking a sorting of SOC deposits into account (Hoffmann et al., 2013).

5. Conclusions

In this modelling study, we used a modified version of the coupled soil erosion and C turnover model SPEROS-C to analyse the effects of the episodic nature of water erosion processes, associated erosion magnitude-specific C enrichment during interrill erosion and C depletion during deposition upon lateral and vertical C fluxes within a small catchment. The following conclusions can be drawn from this modelling study: (i) Assuming that robust conceptual erosion models are the best available tools to analyse long-term (decades to centuries) effects of SOC redistribution on C fluxes, since more process-oriented erosion models need to be intensively parameterised for such long-term studies, it seems to be essential to conceptually integrate erosion variability, enrichment of SOC due to selective erosion and deposition into these models. In general, the approach used in this study illustrates the potential effects of these processes. However, not enough is known on how to integrate and parameterise these processes in real catchments. (ii) Ignoring the episodic nature of erosion might be less critical for a comparison between modelled erosion patterns and measured SOC patterns, but cannot be ignored when the variability of catchment outputs is required. (iii) C enrichment during erosion is especially important for small erosion events (again underlining the importance of taking erosion variability into account). Hence, the effects of terrestrial C input into aquatic systems due to small erosion events should demand more attention. In general, C delivery is amplified when enrichment during erosion and depletion during deposition are combined. (iv) Besides SOC delivery, the processes included into SPEROS-C also substantially change the modelled vertical C fluxes and hence also overall resulting SOC patterns. The modelling study especially underlines the importance of combining C enrichment due to (interrill) erosion and C depletion due to deposition to understand the C fluxes and SOC contents at depositional sites. This kind of 'double-sorting' of C associated with different particle size or density fractions is also essential to understanding long-term C stability at depositional sites.

References

Afshar, F.A., Ayoubi, S., Jalalian, A., 2010. Soil redistribution rate and its relationship with soil organic carbon and total nitrogen using Cs-137 technique in a cultivated complex hillslope in western Iran. J. Environ. Radioact. 101 (8), 606–614.

Andrén, O., Kätterer, T., 1997. ICBM: the introductory carbon balance model for exploration of soil carbon balances. Ecol. Appl. 7 (4), 1226–1236.

Auerswald, K., Weigand, S., 1999. Eintrag und Freisetzung von P durch Erosionsmaterial in Oberflächengewässern. VDLUFA-Schriftenreihe 50, 37–54.

Berhe, A.A., Kleber, M., 2013. Erosion, deposition, and the persistence of soil organic matter: mechanistic considerations and problems with terminology. Earth Surf. Process. Landforms 38, 908–912.

Berhe, A.A., Harden, J.W., Torn, M.S., Harte, J., 2008. Linking soil organic matter dynamics and erosion-induced terrestrial carbon sequestration at different landform positions. J. Geophys. Res. 113, G04039.

Bremenfeld, S., Fiener, P., Govers, G., 2013. Effects of interrill erosion, soil crusting and soil aggregate breakdown on in situ CO_2 effluxes. Catena 104, 14–20.

Coleman, K., Jenkinson, D.S., 2008. ROTH-C-26.3. A Model for the Turnover of Carbon in Soil. Model Description and Windows User Guide. http://www.rothamsted.bbsrc.ac.uk/aen/carbon/rothc.htm.

Dlugoß, V., Fiener, P., Schneider, K., 2010. Layer-specific analysis and spatial prediction of soil organic carbon using terrain attributes and erosion modeling. Soil Sci. Soc. Am. J. 74 (3), 922–935.

Dlugoß, V., Fiener, P., Van Oost, K., Schneider, K., 2012. Model based analysis of lateral and vertical soil C fluxes induced by soil redistribution processes in a small agricultural watershed. Earth Surf. Process. Landforms 37 (2), 193–208.

Doetterl, S., Stevens, A., Van Oost, K., Quine, T.A., Van Wesemael, B., 2013. Spatially-explicit regional-scale prediction of soil organic carbon stocks in cropland using environmental variables and mixed model approaches. Geoderma 204–205, 31–42.

Dymond, J.R., 2010. Soil erosion in New Zealand is a net sink of CO_2. Earth Surf. Process. Landforms 35 (15), 1763–1772.

FAO, 1998. World Reference Base for Soil Resources. United Nations, Rome.

Fiener, P., Auerswald, K., 2007. Rotation effects of potato, maize and winter wheat on soil erosion by water. Soil Sci. Soc. Am. J. 71 (6), 1919–1925.

Fiener, P., Govers, G., Van Oost, K., 2008. Evaluation of a dynamic multi-class sediment transport model in a catchment under soil-conservation agriculture. Earth Surf. Process. Landforms 33, 1639–1660.

Fiener, P., Dlugoß, V., Korres, W., Schneider, K., 2012. Spatial variability of soil respiration in a small agricultural watershed — are patterns of soil redistribution important? Catena 94, 3–16.

Fiener, P., Neuhaus, P., Botschek, J., 2013. Long-term trends in rainfall erosivity — analysis of high resolution precipitation time series (1937–2007) from Western Germany. Agric. For. Meteorol. 171–172, 115–123.

Govers, G., Vandaele, K., Desmet, P., Poesen, J., Bunte, K., 1994. The role of tillage in soil redistribution on hillslopes. Eur. J. Soil Sci. 45, 469–478.

Hairsine, P.B., Beuselinck, L., Sander, G.C., 2002. Sediment transport through an area of net deposition. Water Resour. Res. 38 (6) (Art. No. 1086 JUN).

Harden, J.W., Sharpe, J.M., Parton, W.J., Ojima, D.S., Fries, T.L., Huntington, T.G., Dabney, S.M., 1999. Dynamic replacement and loss of soil carbon by eroding cropland. Glob. Biogeochem. Cycles 13 (4), 885–901.

Hoffmann, T., Schlummer, M., Notebaert, B., Verstraeten, G., Korup, O., 2013. Carbon burial in soil sediments from Holocene agricultural erosion, Central Europe. Glob. Biogeochem. Cycles 27 (3), 828–835.

Hu, Y., Kuhn, N.J., 2014. Aggregates reduce transport distance of soil organic carbon: are our balances correct? Biogeosci. 11, 6209–6219.

Kuhn, N.J., Armstrong, E.K., Ling, A.C., Connolly, K.L., Heckrath, G., 2010. Interrill erosion of carbon and phosphorus from conventionally and organically farmed Devon silt soils. Catena 91, 94–103.

Laflen, J.M., Elliot, W.J., Flanagan, D.C., Meyer, C.R., Nearing, M.A., 1997. WEPP-predicting water erosion using a process-based model. J. Soil Water Conserv. 52, 96–102.

Martinez, C., Hancock, G.R., Kalma, J.D., 2010. Relationships between Cs-137 and soil organic carbon (SOC) in cultivated and never-cultivated soils: an Australian example. Geoderma 158 (3–4), 137–147.

Meersmans, J., Van Wesemael, B., Goidts, E., Van Molle, M., De Baets, S., De Ridder, F., 2011. Spatial analysis of soil organic carbon evolution in Belgian croplands and grasslands, 1960–2006. Glob. Change Biol. 17 (1), 466–479.

Menzel, R.G., 1980. Enrichment ratios for water quality modeling. In: Knisel, W.G. (Ed.), CREAMS. USDA Cons. Res. Rep, Washington DC, pp. 486–492.

Nadeu, E., Gobin, A., Fiener, P., Van Wesemael, B., Van Oost, K., 2015. Modelling the impact of agricultural management on soil carbon stocks at the regional scale: the role of lateral fluxes. Glob. Change Biol. http://dx.doi.org/10.1111/gcb.12889.

Nearing, M.A., Govers, G., Norton, D.L., 1999. Variability in soil erosion data from replicated plots. Soil Sci. Soc. Am. J. 63, 1829–1835.

Polyakov, V.O., Lal, R., 2004. Soil erosion and carbon dynamics under simulated rainfall. Soil Sci. 169 (8), 590–599.

Preston, N.J., 2001. Geomorphic Response to Environmental Change: The Imprint of Deforestation and Agricultural Land Use on the Contemporary Landscape of the Pleiser Hügelland (PhD Thesis). Rheinische Friedrich-Wilhelms-Universität, Bonn, Germany.

Quine, T.A., Van Oost, K., 2007. Quantifying carbon sequestration as a result of soil erosion and deposition: restrospective assessment using caesium-137 and carbon inventories. Glob. Change Biol. 13, 2610–2625.

Quinton, J.N., Govers, G., Van Oost, K., Bardgett, R.D., 2010. The impact of agricultural soil erosion on biogeochemical cycling. Nat. Geosci. 3, 311–314.

Renard, K.G., Foster, G.R., Weesies, G.A., McCool, D.K., Yoder, D.C., 1996. Predicting soil erosion by water: a guide to conservation planning with the Revised Universal Soil Loss Equation (RUSLE). Agricultural Handbook 703. USDA-ARS, Washington DC.

Rosenbloom, N.A., Doney, S.C., Schimel, D.S., 2001. Geomorphic evolution of soil texture and organic matter in eroding landscapes. Glob. Biogeochem. Cycles 15 (2), 365–381.

Ruysschaert, G., Poesen, J., Verstraeten, G., Govers, G., 2004. Soil loss due to crop harvesting: significance and determining factors. Prog. Phys. Geogr. 4, 467–501.

Ruysschaert, G., Poesen, J., Verstraeten, G., Govers, G., 2005. Interannual variation of soil losses due to sugar beet harvesting in West Europe. Agric. Ecosyst. Environ. 107, 317–329.

Schiettecatte, W., Gabriels, D., Cornelis, W., Hofman, G., 2008a. Impact of deposition on the enrichment of organic carbon in eroded sediment. Catena 72, 340–347.

Schiettecatte, W., Gabriels, D., Cornelis, W.M., Hofman, G., 2008b. Enrichment of organic carbon in sediment transport by interrill and rill erosion processes. Soil Sci. Soc. Am. J. 72 (1), 50–55.

Schmidt, J.V., Werner, M., Michael, A., 1999. Application of the EROSION 3D model to the CATSOP watershed, the Netherlands. Catena 37, 449–456.

Sharpley, A.N., 1985. The selective erosion of plant nutrients in runoff. Soil Sci. Soc. Am. J. 49, 1527–1534.

Skjemstad, J.O., Spouncer, L.R., Cowie, B., Swift, R.S., 2004. Calibration of the Rothamsted organic carbon turnover model (RothC ver. 26.3), using measurable soil organic carbon pools. Aust. J. Soil Res. 42, 79–88.

Stallard, R., 1998. Terrestrial sedimentation and the carbon cycle: coupling weathering and erosion to carbon burial. Glob. Biogeochem. Cycles 12 (2), 231–257.

Van Hemelryck, H., Fiener, P., Van Oost, K., Govers, G., Merckx, R., 2010a. The effect of soil redistribution on soil organic carbon: an experimental study. Biogeosciences 7, 3971–3986.

Van Hemelryck, H., Govers, G., Van Oost, K., Merckx, R., 2010b. Evaluating the impact of soil redistribution on the in situ mineralization of soil organic carbon. Earth Surf. Process. Landforms 36, 427–438.

Van Oost, K., Govers, G., Quine, T., Heckarth, G., Olesen, J.E., De Gryze, S., Merckx, R., 2005a. Landscape-scale modeling of carbon cycling under the impact of soil redistribution: the role of tillage erosion. Glob. Biogeochem. Cycles 19, GB4014.

Van Oost, K., Quine, T., Govers, G., Heckrath, G., 2005b. Modeling soil erosion induced carbon fluxes between soil and atmosphere on agricultural land using SPEROS-C. In: Roose, E.J., Lal, R., Feller, C., Barthes, B., Stewart, B.A. (Eds.), Advances in Soil Science. Soil Erosion and Carbon Dynamics. CRC Press, Boca Raton, pp. 37–51.

Van Oost, K., Quine, T.A., Govers, G., De Gryze, S., Six, J., Harden, J.W., Ritchie, J.C., McCarty, G.W., Heckrath, G., Kosmas, C., Giraldez, J.V., Marques da Silva, J.R., Merckx, R., 2007. The impact of agricultural soil erosion on the global carbon cycle. Science 318, 626–629.

Virto, I., Barré, P., Chenu, C., 2008. Microaggregation and organic matter storage at the silt-size scale. Geoderma 146, 326–335.

Wang, Z., Govers, G., Steegen, A., Clymans, W., Van den Putte, A., Langhans, C., Merckx, R., Van Oost, K., 2010. Catchment-scale carbon redistribution and delivery by water erosion in an intensively cultivated area. Geomorphology 124 (1–2), 65–74.

Wang, Z., Govers, G., Van Oost, K., Clymans, W., Van den Putte, A., Merckx, R., 2013. Soil organic carbon mobilization by interrill erosion: insights from size fractions. J. Geophys. Res. 118 (2), 348–360.

Wang, X., Cammeraat, E.L.H., Romeijn, P., Kalbitz, K., 2014. Soil organic carbon redistribution by water erosion — the role of CO_2 emissions for the carbon budget. PLoS One 9 (5).

Wischmeier, W.H., Smith, D.D., 1960. A universal soil-loss equation to guide conservation farm planning. Madison, Wisc. Proceedings of 7th Intern. Congress of Soil Science, pp. 418–425.